Supplementary Information

Synthesis of cubic transition-metal networks from polymer cubosome templates

Heelim Lee,[a] DoKyun Kim,[a] Hyunji Ma,[a] and Kyoung Taek Kim*[a]
[a]Department of Chemistry, Seoul National University, Seoul 08826, Korea

*Correspondence to: ktkim72@snu.ac.kr

CONTENTS

1. Materials and Methods

Materials. Unless otherwise noted, all reagents and chemicals were purchased from Sigma Aldrich, Alfa Aesar, and TCI and used as received. Styrene monomer was purified by basic alumina column before use. Dichloromethane (MC) was dried over CaH_2 under N_2. Tetrahydrofuran (THF) was refluxed over a mixture of Na and benzophenone under N_2 and distilled before use. Deionized water was purged with N_2 before use.

Methods. ^{1}H NMR spectra were recorded on Agilent 500-MR DD2 Magnetic Resonance System and Varian/Oxford AS-500 using CD2Cl2 as solvent and internal standards.

Molecular weights and dispersity D of block copolymers were measured by Agilent 1260 Infinity gel permeation chromatography (GPC) system equipped with a PL gel 5 μm MiniMIX-D column (Agilent Technologies) and differential refractive index detectors. THF was used as an eluent with a flow rate of 1.0 mL min^{-1} at 35 °C and the analytical sample was filtered by using PTFE filter before injection. A PS standard kit (Agilent Technologies) was used for calibration.

Scanning electron microscopy (SEM) was performed on a Hitachi S-4300 operating at 15 kV. Field emission SEM (FESEM) was performed on a Zeiss Supra 55VP operating at 2 kV. Dried polymer cubosomes were placed on a conductive carbon tape and then coated with Pt by using a Hitachi E-1030 ion sputter coater (20 mA, 60s).

Transmission electron microscopy (TEM) was performed on a Hitachi 7600 operating at 100 kV and a JEOL JEM-3010 operating at 300 kV. TEM specimens were prepared by placing a drop of solution on a carbon-coated Copper grid (200 mesh, EM science). After 30 minutes, the remaining solution on a grid was removed with a filter

paper, and the grid was dried overnight. The morphologies of polymer and templated metal mesostructures were measured by analyzing TEM images.

Energy dispersive X-ray spectroscopy (EDXS) was recorded to determine the chemical identity of the metal specimen. Powder X-ray diffraction (XRD) patterns of all the products obtained in this work were recorded with a Bruker D8 Advance X-ray powder diffractometer with monochromatized Cu Kα radiation (λ = 1.5406 Å).

Synchrotron small angle X-ray scattering (SAXS) data were obtained on the 6D SAXS beam line at Pohang acceleration laboratory in Korea (PLS-II, 3.0 GeV). The sample-to-detector distance (SDD) was 3.5 m. The concentrated suspension of the PCs was dried for 24 h in a freeze-dryer. Ti-SBA-15 was used as standard sample and scattering spectra of powder samples were taken in a transmission mode at room temperature (11.6 keV).

the magnetic susceptibility of DD Ni cubic networks was taken in a MPMS- 2000 SQUID Amplifier control electronics (1.9 to 400 K).

2. Synthesis of branched-linear poly(ethylene glycol$_m$)$_3$-*block*-poly(styrene) (PEG$_m$)$_3$-*b*-PS$_n$.

(PEG$_m$)$_3$-*b*-PS$_n$ was synthesized according to the previously reported method[1–2]. In brief description, a PEG-linked macroinitiator was synthesized by tethering three PEG chains to a 3,4,5-trihydroxybenzyl ester core (Scheme S1). Using the PEG-linked macroinitiator, polymers with three different length of the PEG blocks were prepared by atomic transfer radical polymerization (ATRP) at 100^{o}C with styrene as a monomer (Scheme S2). Polymer growth was monitored by gel permeation chromatography (GPC) at different time points.

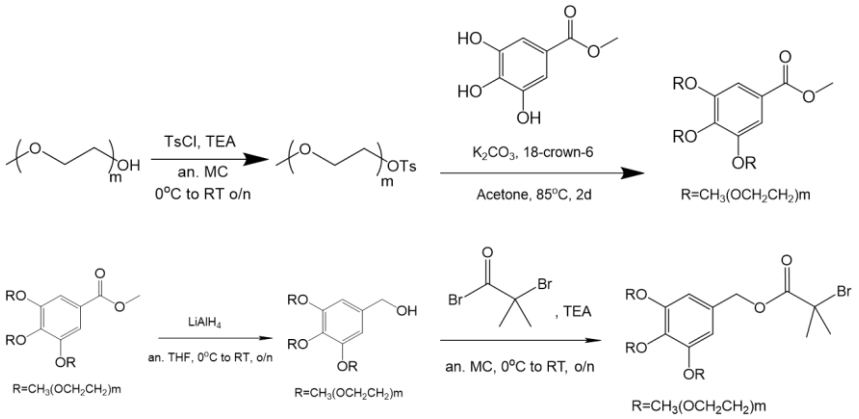

Scheme S1. Synthetic scheme for preparing $(PEG_m)_3$-linked ATRP macroinitiator for the synthesis of $(PEG_m)_3$-*b*-PS_n.

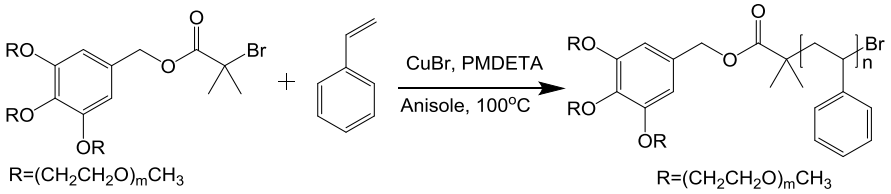

Scheme S2. Synthetic scheme for preparing branched-linear $(PEG_m)_3$-*b*-PS_n by atomic transfer radical polymerization (ATRP).

2.2 Characterization of the prepared polymers.

The number average molecular weight and molecular weight distribution was determined by GPC (THF, 35°C, 1 mL min^{-1} flow rate) calibrated with PS standards. The number average degree of polymerization of PS block was determined by ^{1}H-NMR integration. The molecular weight ratio of the PEG domain to that of the PS block (M_n(PEG550$_3$) = 1,650 g/mol; M_n(PEG1K$_3$) = 2,950 g/mol).

Table S1. List of polymers prepared by ATRP.

Polymer	M_n[a] [g/mol]	PDI[a] (M_w/M_n)	DP_n(PS)[b]	Block ratio[c] (f_{PEG}, %)
$PEG550_3$-*b*-PS_{155}	17,200	1.09	155	10.2
$PEG1K_3$-*b*-PS_{304}	77,400	1.13	304	9.34

[a] The number average molecular weight and molecular weight distribution determined by GPC (THF, 35 °C, 1 mL min^{-1} flow rate) using PS standards. [b] The number average degree of polymerization of PS block determined by ^1H NMR integration. [c] The molecular weight ratio of the PEG domain to that of the PS block.

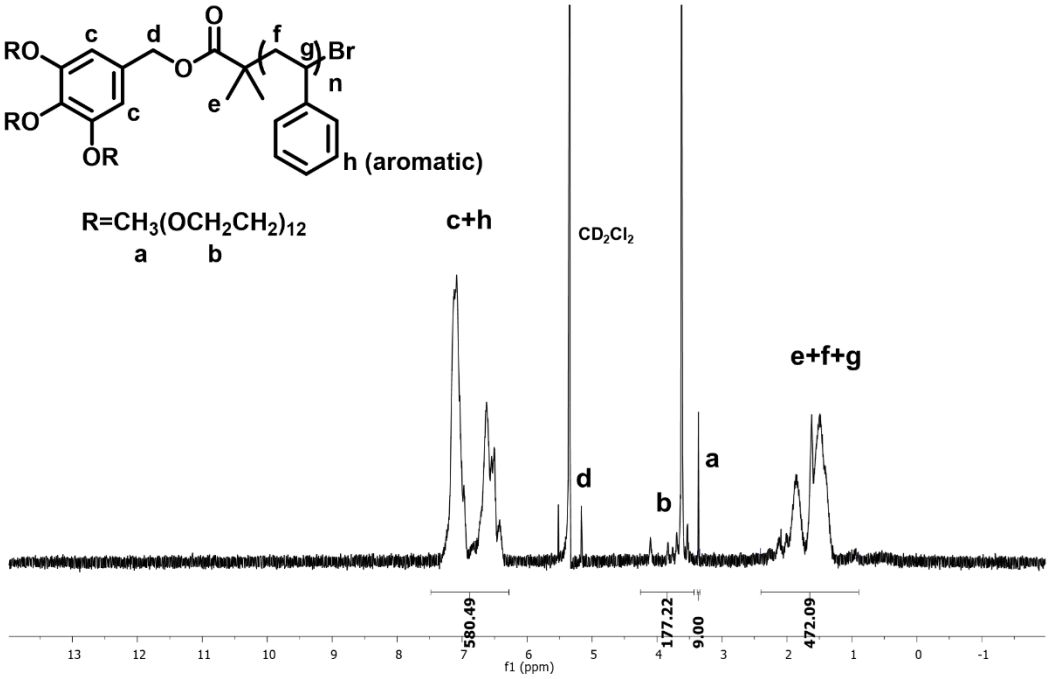

Figure S1. ^1H NMR spectrum of $(PEG550)_3$-*b*-PS_{155} BCP (500 MHz, CD_2Cl_2).

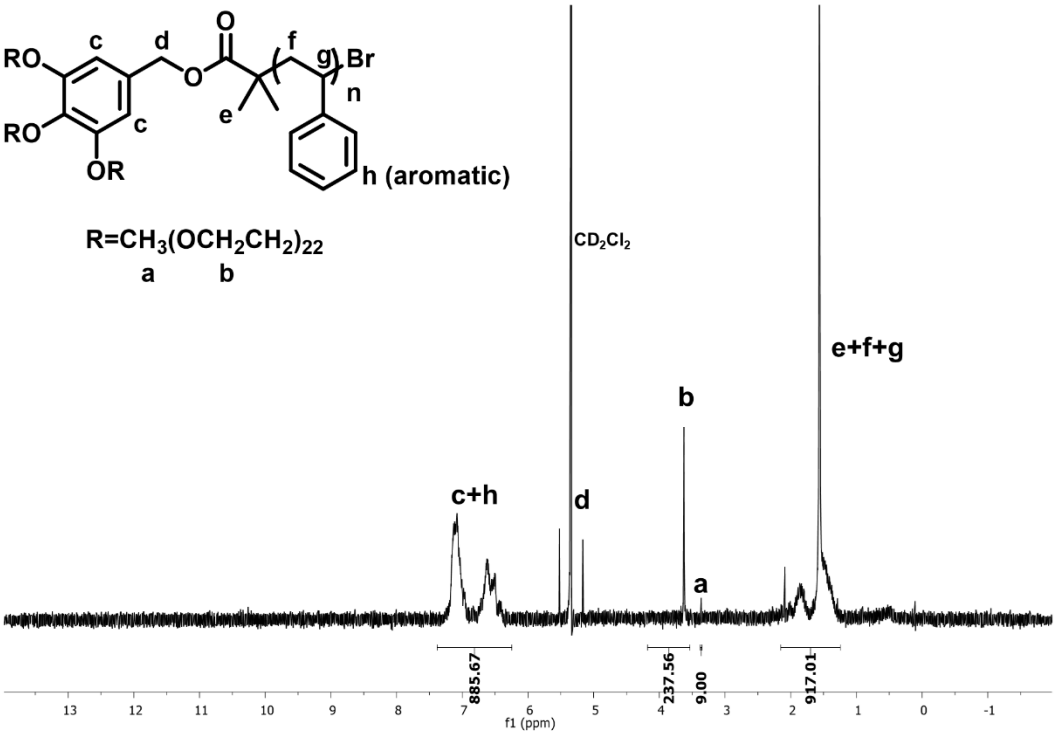

Figure S2. ^1H NMR spectrum of $(PEG1K)_3$-*b*-PS_{304} BCP (500 MHz, CD_2Cl_2).

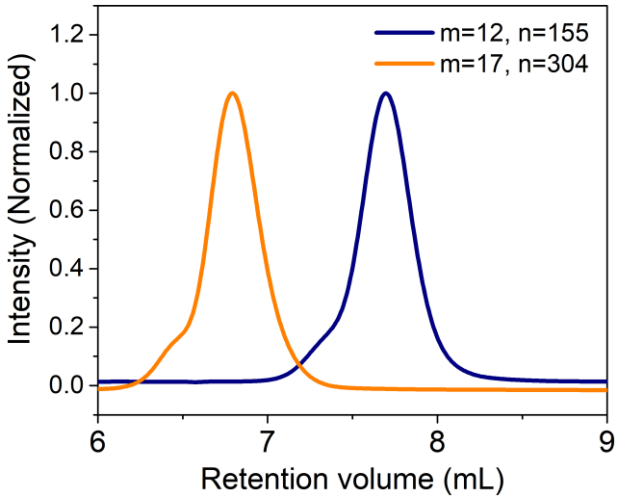

Figure S3. GPC chromatogram of $(PEG550)_3$-*b*-PS_{155} (M_n = 17.2×10^3 g·mol^{-1}) (navy) and $(PEG1K)_3$-*b*-PS_{304} (M_n = 77.4×10^3 g·mol^{-1}) (orange) BCPs. Mobile phase: THF, 35°C, 1 mL min^{-1} flow rate. Calibrated with with PS standards.

3. Self-assembly of $(PEG_m)_3$-*b*-PS_n into bicontinuous inverse cubic mesophases.

3.1 Solution self-assembly of $(PEG550)_3$-*b*-PS_m into colloidal inverse cubic mesophase membranes (cubosomes).

Cubosomes were prepared by solution self-assembly by co-solvent method[1-2]. First, a polymer solution (0.5-1.0 wt%) was prepared by dissolving the polymer in 1,4-dioxane in a 20 mL screw cap vial. The polymer solution was stirred with a magnetic stirring bar for at least 15 minutes to ensure homogeneity. Then, deionized water was slowly added into the polymer solution by using a programmable syringe pump. After four hours, the resulting suspension was dialyzed against water for 24 hours using dialysis bag (molecular weight cutoff = 12–13 kDa, SpectraPor) to allow slow removal of the organic solvent. Finally, cubosomes were isolated by centrifugation at 14000 g for 6 minutes.

3.2 Self-assembly of $(PEG550)_3$-*b*-PS_m into bicontinuous inverse cubic monoliths by solvent diffusion-evaporation mediated self-assembly (SDEMS).

Inverse cubic monoliths were prepared by solvent diffusion-evaporation mediated self-assembly (SDEMS)[1-2]. First, a polymer solution (12.0-13.0 wt%) was prepared by dissolving the polymer in 1,4-dioxane. The polymer solution was stirred and shaken for at least two hours to ensure homogeneity. Meanwhile, a 50% relative humidity (RH) chamber was prepared by placing 20 mL of 50% volumetric mixture of 1,4-dioxane and deionized water in a screw cap glass chamber. A 20 mL screw vial was placed inside of the chamber as a foundation, where two clean glass plates cut into 0.6 cm by 0.6 cm were fixed onto. 10-20 µL of the polymer solution was carefully placed onto the glass plates. After two to four hours, the glass plates were removed from the chamber and were placed in deionized water for the dialysis against deionized water. The medium was refreshed once in few hours for two days to ensure removal of the organic solvent. The resulting monoliths were isolated and dried under atmospheric pressure at room temperature.

3.3 SEM and SAXS analysis of polymer cubosomes

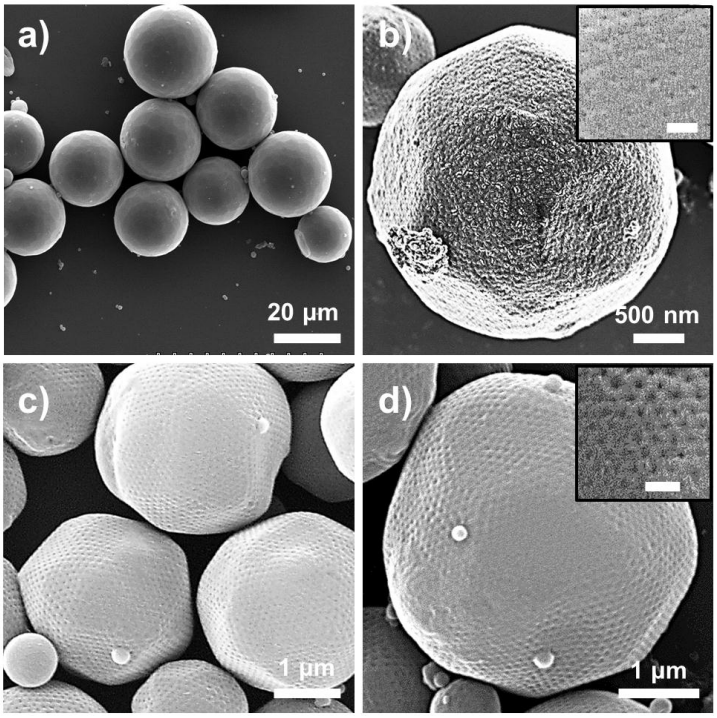

Figure S4. (a, b) FESEM images of $(PEG550)_3$-*b*-PS_{155} polymer cubosomes. (Inset) Periodic pores on the (111) plane are shown. Scale bar=100 nm. (c, d) FESEM images of $(PEG1K)_3$-*b*-PS_{304} polymer cubosomes. (Inset) Periodic pores on the (111) plane are shown. Scale bar=100 nm.

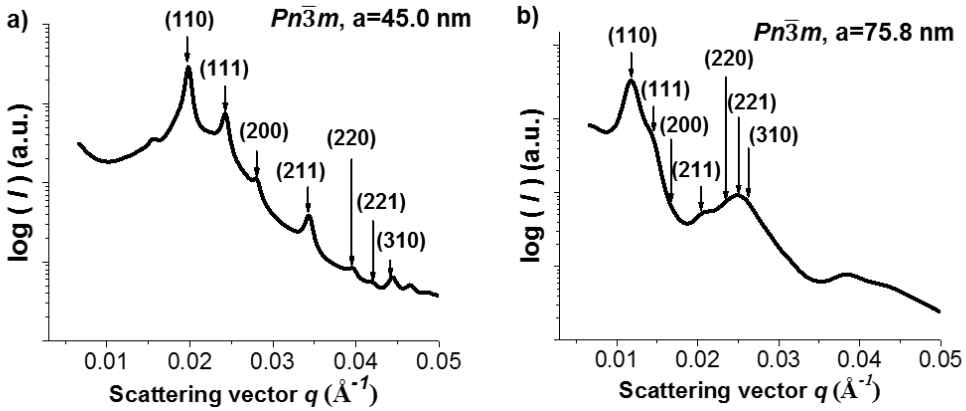

Figure S5. SAXS analysis of (a) $(PEG550)_3$-*b*-PS_{155} polymer cubosome (*Pn3m*, *a* = 45.0 nm); (b) $(PEG1K)_3$-*b*-PS_{304} polymer cubosome (Pn3m, a=75.8 nm).

4. Templated synthesis of single and double nickel networks

4.1 Procedures of electroless plating of nickel

The procedure was adapted from the literature with slight modification[3]. First, a pale orange solution containing palladium (II) chloride ($PdCl_2$, Sigma-Aldrich, 80 – 4,000 mg mL^{-1}) in methanol and 10% 1N hydrogen chloride solution was prepared. Then, a mesoporous inverse cubic $(PEG)_3$-*b*-PS template was immersed in the prepared Pd^{2+} solution. After 3 hours, the polymer template was taken out from the Pd^{2+} solution and was rinsed thoroughly with DI water and ethanol several times. Then, the rinsed template was placed in a 50% hydrazinium hydroxide solution ($N_2H_4{\cdot}H_2O$, Alfa Aesar) overnight. The template was taken out and was rinsed thoroughly with DI water and ethanol several times. Then, the template was immersed in a dark blue aqueous solution containing nickel (II) chloride hexahydrate

($NiCl_2 \cdot 6H_2O$, Sigma-Aldrich, 54.65 mg mL^{-1}), hydrazinium hydroxide ($N_2H_4 \cdot H_2O$, Alfa Aesar, 196.7 mg mL^{-1}), 35% ammonia solution, and methanol. At different time of growth, the Ni@template was taken out, rinsed with DI water and ethanol several times. The isolated Ni@template was placed in an organic solution, where the polymer template was dissolved and the Ni networks were retrieved by a magnet.

Since the interaction between the polymer template and the metal precursors is weak compared to the other traditional metal-binding functional groups, different conditions were tested to optimize number of growing sites, length scale of growth, and time of growth without generating free metal particles in the background.

4.2 Adjusting the concentration of palladium

In order to increase the number of growing sites, methanolic solutions of 80 mg mL^{-1} to 4,000 mg mL^{-1} $PdCl_2$ were prepared. A polymer template was immersed in different conditions while keeping the reduction and nickel growth conditions the same (33mM Ni^{2+}, molar ratio of Ni and hydrazine=12). Samples were grown for two days, isolated, and were analyzed under SEM (Fig. S8). With same conditions, the templates were allowed to grow for 5 days (Fig. S9).

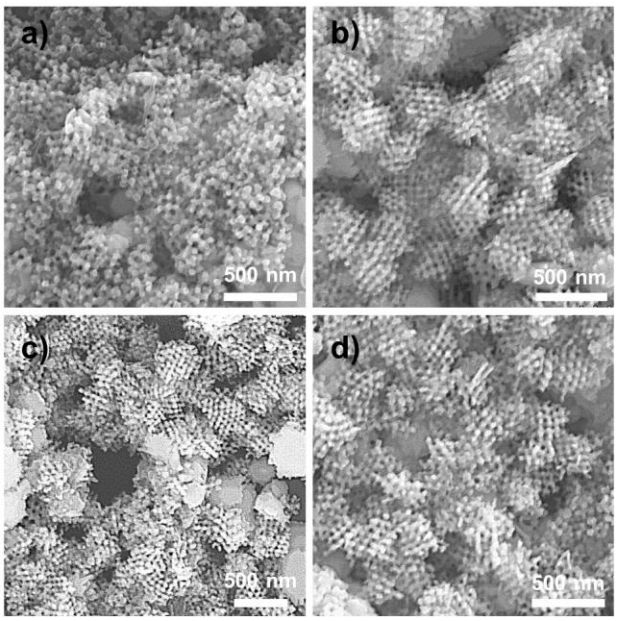

Figure S6. SEM images of nickel networks activated with different Pd^{2+} concentrations after growth in an identical Ni plating solution (33mM Ni^{2+}, molar ratio of Ni and hydrazine=12) for 2 days. a) 496 mg mL^{-1} Pd^{2+}. Domain size is 283 nm; b) 606 mg mL^{-1} Pd^{2+}. Domain size is 340 nm; c) 726 mg mL^{-1} Pd^{2+}. Domain size is 380 nm; d) 800 mg mL^{-1} Pd^{2+}. Domain size is 320 nm.

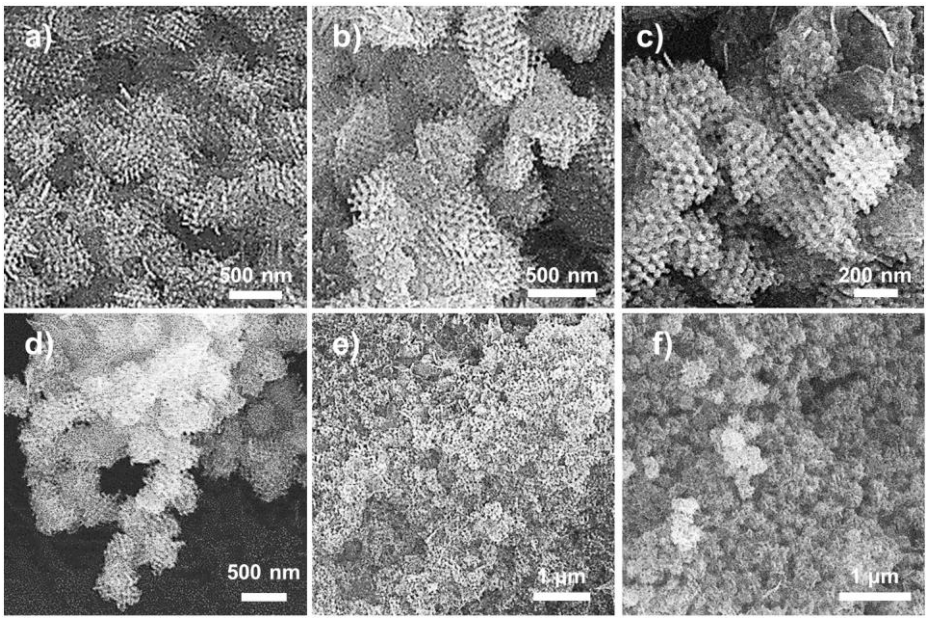

Figure S7. SEM images of nickel networks obtained at different Pd^{2+} concentrations after growth in an identical Ni plating solution (33mM Ni^{2+}, molar ratio of Ni and

hydrazine=12) for 5 days. a) 606 mg mL^{-1} Pd^{2+}. Domain size is 450 nm; b) 800 mg mL^{-1} Pd^{2+}. Domain size is 478 nm; c) 1,500 mg mL^{-1} Pd^{2+}. Domain size is 340 nm; d) 2,000 mg mL^{-1} Pd^{2+}. Domain size is 434 nm; e) 3,000 mg mL^{-1} Pd^{2+}. f) 4,000 mg mL^{-1} Pd^{2+}.

Increasing the concentration of palladium precursors from 80 mg mL^{-1} to 4,000 mg mL^{-1} increased the density of growing sites and greater yield, but the overall size of the nickel obtained stopped growing at about 300 nanometers in size. Higher concentration of palladium ions increase the number of growing centers to coalesce together, thereby increasing the overall size of the products. Also, the dissolution of Pd^{2+} in methanol becomes problematic at higher concentrations. Thus, 4,000 mg mL^{-1} Pd^{2+} solution was used for further synthesis.

4.3 Adjusting the molar ratio of Ni and hydrazine

Also, the molar ratio of the reductant to the divalent nickel precursors in the nickel plating solution was adjusted to increase the efficiency of the synthesis over a greater length scale. The nickel ions should be able to reach the growing fronts in throughout the entire template without being reduced to atomic nickel. The Pourbaix diagram provides thermodynamic transition metal species present in a specific condition (i. e. electrochemical potential, pH, temperature, etc.), and adjusting the molar ratio of the reductant to the divalent nickel ion is one way to control the rate of growth. Therefore, nickel plating solutions with different molar ratio of the reductant

to Ni^{2+} were prepared. Polymer templates were placed in different nickel plating solutions and were grown for five days at all the other equal conditions (33 mM Ni^{2+}).

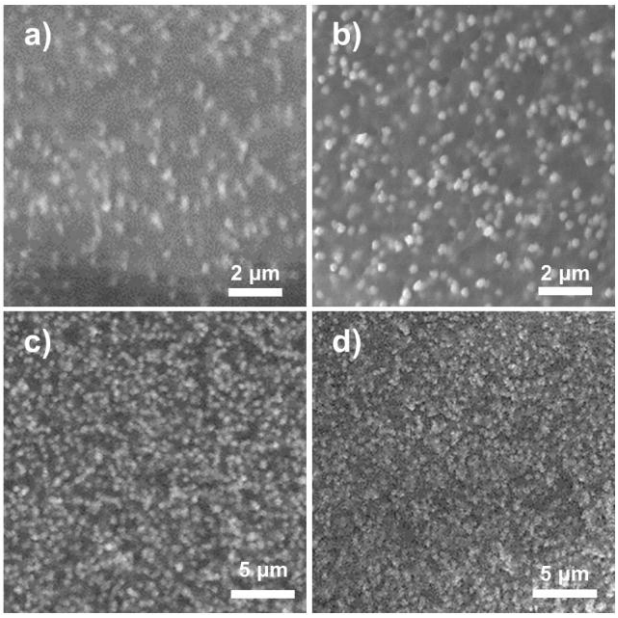

Figure S8. SEM images of the cross-section of the growing Ni@monolith in Ni plating solutions of 33 mM Ni^{2+} and different conditions. a) 1,500 mg mL^{-1} Pd^{2+}, molar ratio of Ni and hydrazine=18. b) 3,000 mg mL^{-1} Pd^{2+}, molar ratio of Ni and hydrazine=18. c) 2,000 mg mL^{-1} Pd^{2+}, molar ratio of Ni and hydrazine=48. d) 4,000 mg mL^{-1} Pd^{2+}, molar ratio of Ni and hydrazine=48.

4.4 Adjusting the concentration of Ni^{2+}

Also, the concentration of the nickel precursor in the nickel plating solutions were adjusted to achieve robust synthesis of nickel networks over a large area.

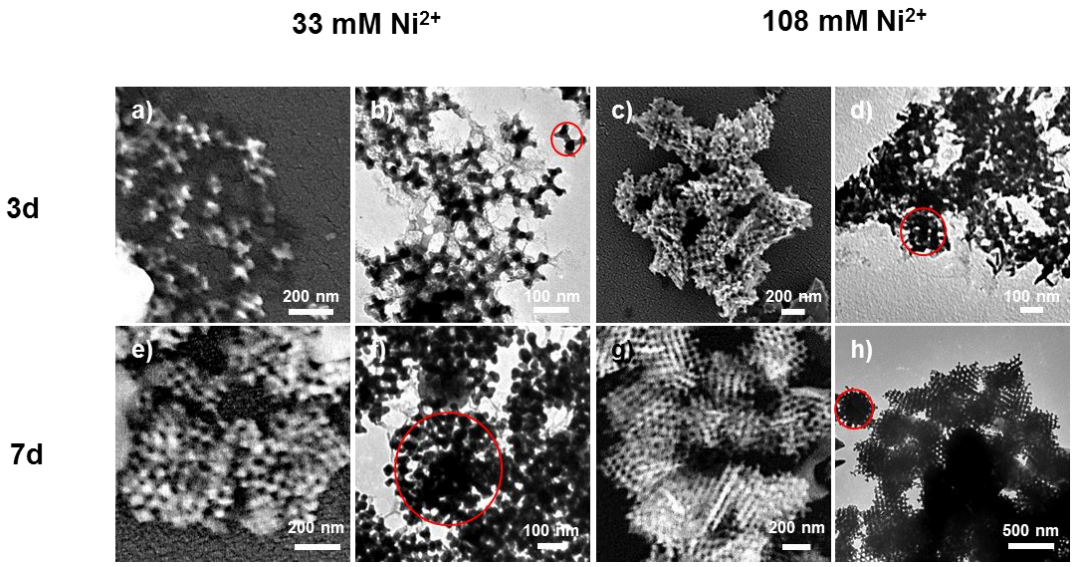

Figure S9. SEM and TEM images of the nickel networks obtained at different Ni^{2+} concentrations after seeding in an identical Pd solution (22.5 mM Pd^{2+}, molar ratio of Ni and hydrazine=12) for 3 days (first row) or 7 days (second row). a, b) 33 mM Ni^{2+}. Domain size is 87.5 nm; c, d) 108 mM Ni^{2+}. Domain size is 200 nm; e, f) 33 mM Ni^{2+}. Domain size is 374 nm; g, h) 108 mM Ni^{2+}. Domain size is 403 nm.

4.5 Adjusting the volume of Ni plating solution

Adjusting the palladium concentrations, nickel concentrations, molar ratio of the nickel precursor to hydrazine did not yield monolithic Ni network. In order to obtain

monolithic Ni network over 200 microns of thickness, the volume of the plating solution was increased to 100 mL and 200 mL.

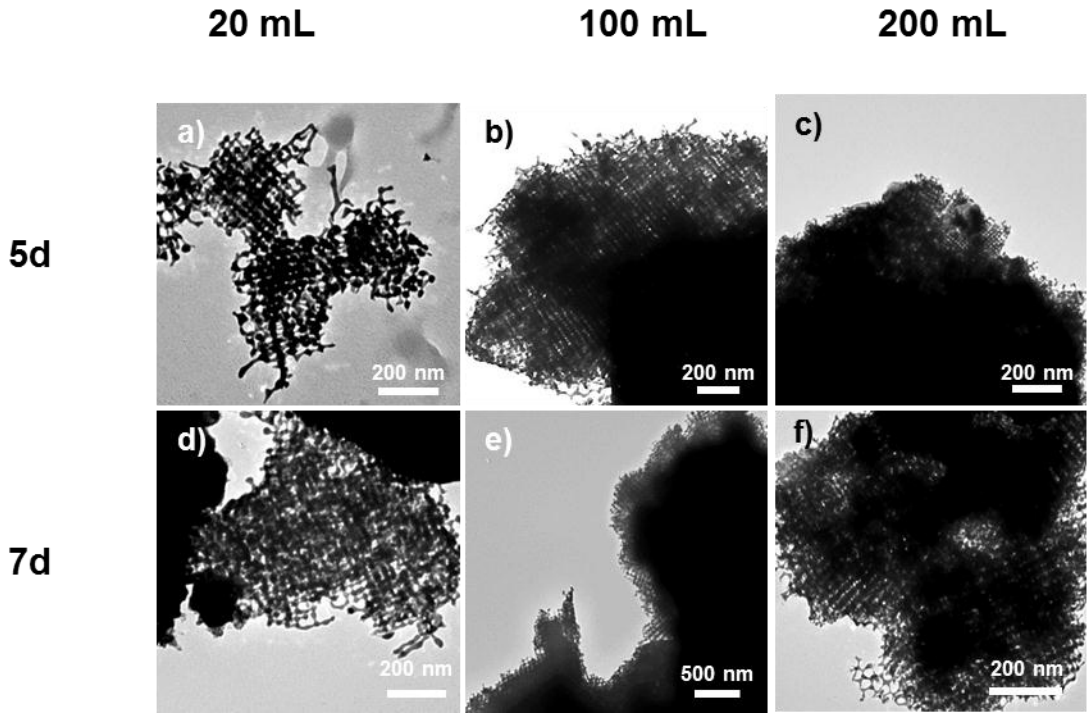

Figure S10. TEM images of the nickel networks grown in different volume of Ni plating solution for 5 days (first row) or 7 days (second row). All other conditions were the same (4,000 mg mL^{-1} Pd^{2+}, 108 mM Ni^{2+}, molar ratio of Ni and hydrazine=12).

4.6 Calculation of lattice parameters from electron microscope images

From high-resolution EM images, the lattice parameters were estimated by drawing skeletal unit cells of the corresponding single (*Fd3m*) or double (*Pn3m*) diamond lattices. For the analysis of the right lattice, two rhombuses of an equal size were placed onto the EM images showing the (111) planes of *Pn3m* or *Fd3m*. First, the vertices of one rhombus was fitted to match the lattice points of the single diamond lattice. Then, the fitted rhombus was copied and the copied rhombus was shifted to match the centers of the pores (*Fd3m*) or the centers of the lattice points of the second lattice (*Pn3m*). For *Fd3m*, the length of a side of the rhombus corresponds to the pore-to-pore distance *d*, which is equal to $\frac{\sqrt{2}}{2}\mathbf{a}$. From the value of *d*, lattice parameter *a* was calculated. For *Pn3m*, the length of the rhombus corresponds to the diagonal distance, which is equal to $\sqrt{2}\boldsymbol{a}$. From the value of this length, lattice parameter *a* was calculated.

5. Templated synthesis of single diamond platinum networks

The procedure was adapted from the literature[4].

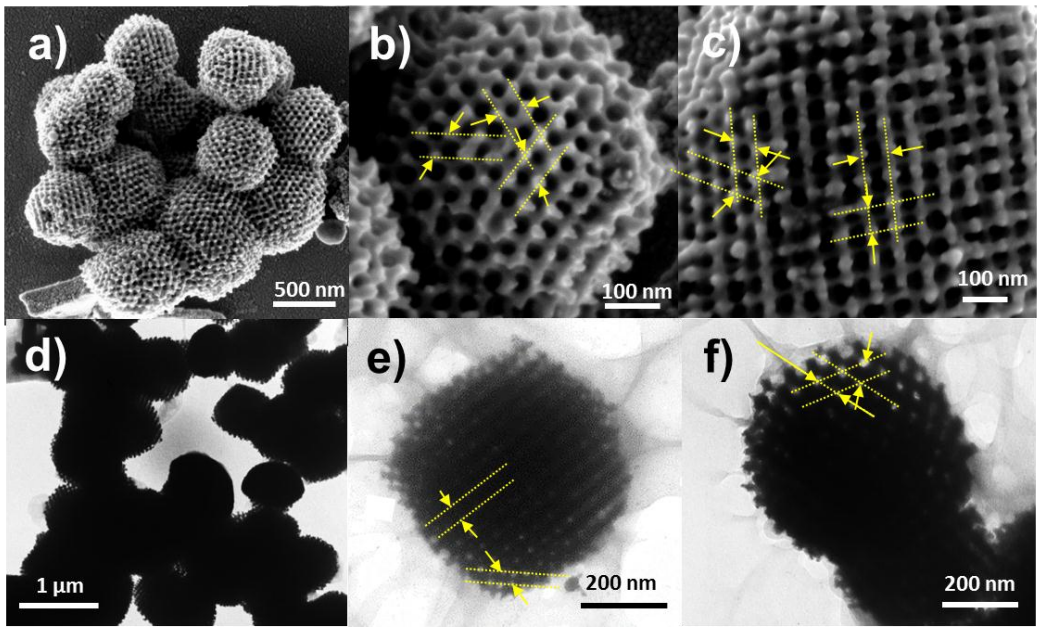

Figure S11. SEM (first row) and TEM (second row) images of platinum networks grown at 3,750 mg mL^{-1} Pt^{2+}, molar ratio of Pt and ascorbic acid=13.7, Ni plating solution=20 mL, for 4 days.

6. SEM and SAXS analysis of cubic mesophase monoliths

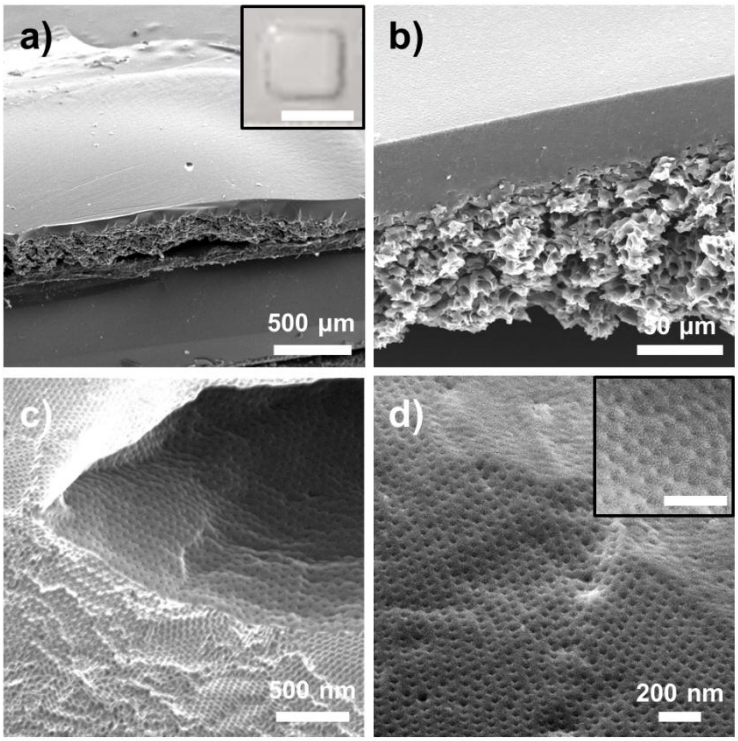

Figure S12. a) SEM image of $(PEG550)_3$-*b*-PS_{155} polymer monolith. a and b) cross-section of the broken monolith. (inset) a photograph of a polymer monolith. Scale bar= 5 mm. c) Surface of the macropores formed at the bottom of the monoliths. d) Top surface. (inset) Only one of its internal channels is open.

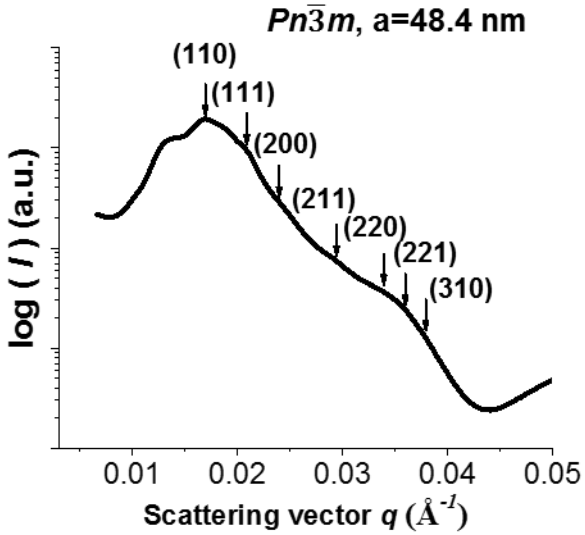

Figure S13. SAXS analysis of $(PEG550)_3$-*b*-PS_{155} cubic monolith as double diamond (*Pn3m*, a=48.4 nm);

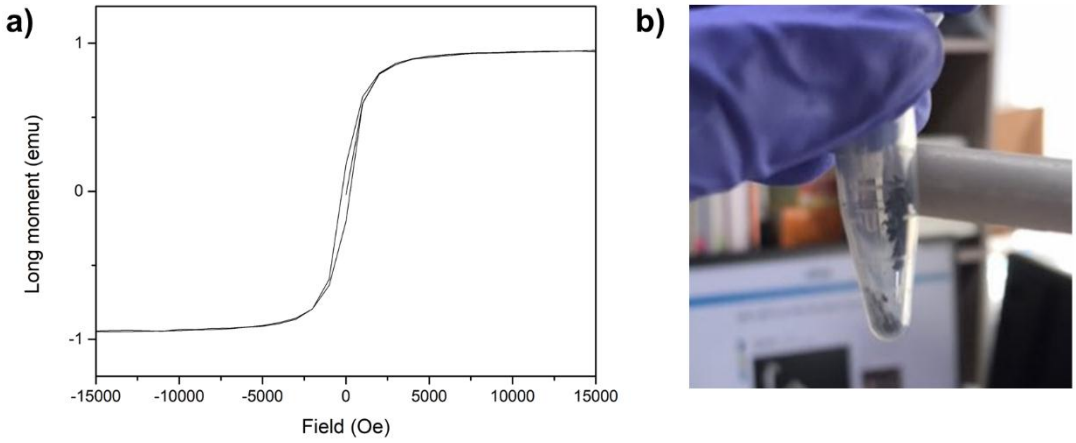

Figure S14. a) The magnetization curves of DD Ni cubic networks at 300K. The narrow hysteresis loop was observed. b) Photo of the DD Ni network indicating the ferromagnetic behavior with the magnet.

7. References

1. T. H. An, Y. La, A. Cho, M. G. Jeong, T. J. Shin, C. Park and K. T. Kim, *ACS Nano*, 2015, **9**, 3084.
2. C. Park, Y. La, T. H. An, H. Y. Jeong, S. Kang, S. H. Joo, H. Ahn, T. J. Shin and K. T. Kim, *Nat. Commun.*, 2015, **6**, 1.
3. H.-Y. Hsueh, Y.-C. Huang, R.-M. Ho, C.-H. Lai, T. Makida and H. Hasegawa, *Adv. Mater.*, 2011, **23**, 3041.
4. C.-F. Cheng, H.-Y. Hsueh, C.-H. Lai, C.-J. Pan, B.-J. Hwang, C.-C. Hu and R.-M. Ho, *NPG Asia Mater.*, 2015, **7**, e170.